RAPID COMMUNICATIONS

PHYSICAL REVIEW B VOLUME 45, NUMBER 23 15 JUNE 1992-I

Quantized conductance in a long silicon inversion wire

Y. S. Tang, G. Jin, J. H. Davies, J. G. Williamson, and C. D. W. Wilkinson
Nanoelectronics Research Center, Department of Electronics and Electrical Engineering, University of Glasgow, Glasgow G12 8QQ, Scotland

(Received 16 December 1991; revised manuscript received 9 March 1992)

Quantized conductance with a step size of less than e^2/h, which increases linearly with increasing perpendicular magnetic field, and resonant tunneling through an impurity state in a long silicon inversion wire have been observed at 4.2 K. This is approximately understood by considering a quantum point contact, an impurity state, and a large gate-voltage-dependent resistor in series.

In the past decade, there has been a lot of progress in introducing concepts in physics and exploiting device applications due to the emergence of quasi-two-dimensional (2D) structures and advances in material growth techniques, such as molecular-beam epitaxy and metal-organic chemical vapor deposition. With the application of electron-beam lithography and reactive ion etching, it has proved possible to introduce another dimensional confinement into a 2D system, such as a silicon inversion layer or a modulation-doped (Al,Ga)As/GaAs heterostructure, to reduce the material dimension further to quasi one dimension (1D, i.e., quantum wires) or zero dimension (0D, i.e., quantum dots). Previous transport measurements on ballistic point contacts[1] in GaAs-based systems have revealed that the 1D conductance is quantized in multiples of $2e^2/h$ in the adiabatic limit, but both recent experimental[2] and theoretical[3] results have shown that, in a real point contact, the minimum quantized conductance step does not necessarily have to be exactly at $2e^2/h$. A 10% variation has been observed experimentally, which has been explained by a 10% change in the transmission probability in the point contact.[2] One may expect to see similar conductance quantization in 1D wires at low temperature where the phase-breaking length L_ϕ is longer than the wire dimensions.[4] Recent studies of silicon inversion wires have seen no clear evidence of quantized conductance.[5] Two papers[6,7] have claimed to see 1D quantized conductance, but have seen no well-defined steps. In this paper, we report an observation of resonant tunneling through an impurity state, which is similar to that reported by McEuen *et al.*,[8] and clear steplike conductance, which has a step size of less than e^2/h, in a long silicon inversion wire. These conductance steps increase linearly with increasing magnetic field, and have been explained approximately by combining a quantum point contact and a large gate-voltage-dependent resistor in the physical picture of the wire, which causes a low observed total conductance in the experiments.

The structure is basically a polycrystalline silicon (poly-Si) gate metal-oxide-semiconductor field-effect transistor (MOSFET) with a long narrow wire gate defined by using electron-beam lithography and reactive ion etching in $SiCl_4$,[9] as shown schematically in Fig. 1(a). The 200-nm-thick heavily arsenic-doped poly-Si wire gate and the p^--type Si ($\rho = 8-16\ \Omega\,\mathrm{cm}$) (100) substrate was separated by 20 nm of thermal oxide [Fig. 1(b)]. The actual gate was a 1.5 μm×70 nm wire with two equally spaced probes [$P1$ and $P2$ in Fig. 1(a)] attached to it, which allow us to carry out four-point transport measurements. The effective mobility of electrons in the channel of a similar device with a wide 2D electron gas region was between 1.4–1.6 $m^2/V\,s$ at 4.2 K.

The experiments were performed in a ^{4}He refrigerator equipped with a superconducting magnet. The conductance measurements were made by using a low-frequency lock-in technique.

Figure 2 shows the gate voltage dependence of both the channel conductance and its derivative measured between probes $P1$ and $P2$ at zero magnetic field. To avoid thermal heating of electrons in the inversion wire, the source-drain voltage was chosen to be 0.1 mV at 4.2 K. It can be clearly seen that steplike quantized conductance was observed with the obvious first step at $\sim 0.6e^2/h$ and a step size of about $0.3e^2/h$. It is more evident from the derivative curve in Fig. 2 that roughly periodic oscillations in dG/dV_G were obtained which reflects the 1D nature of the density of states with changing gate voltage.[6] Similar features were also observed on a separate device of the same type on the same chip. The biggest difference be-

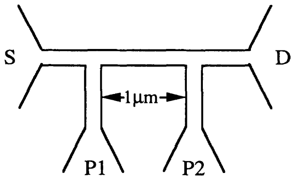

(a) top view

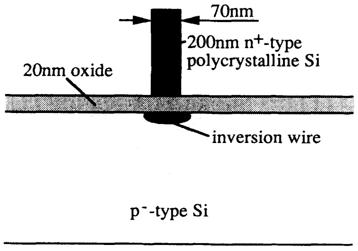

(b) cross section

FIG. 1. Schematic diagram of the device structure.

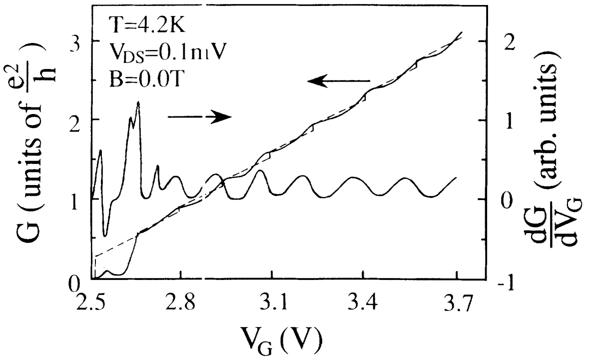

FIG. 2. Gate voltage V_G dependence of the conductance and its derivative in a long narrow inversion wire. Clear steplike behavior has been observed which has a step size of less than e^2/h; the dashed line is a simple fit of Eq. (2) to the experimental $G \sim V_G$ curve. A resonant tunneling peak related to impurity state in the wire is also resolved in the measured curve.

tween our results and the published data on quantum point contacts in modulation-doped 2D electron gas in heterostructures based on III-V compounds, such as a (Al,Ga)As/GaAs system, is that our observed quantized steps in conductance are much smaller than the theoretical value based on an adiabatic approximation, as expressed by Landauer's formula[10] on the multichannel version of 1D conductance G_p in a quantum point contact,

$$G_p=\frac{4e^2}{h}\sum_{\mu,\nu}t_{\mu\nu}^2 , \tag{1}$$

where a factor of 4 accounts for both the spin and valley degeneracies in a (100) silicon system; $t_{\mu\nu}$ is the transmission coefficient; and the summation, representing the total number of transverse modes in the 1D structure in the adiabatic limit, is over all the possible conducting channels, which means that the 1D conductance can only be multiples of a universal constant $4e^2/h$. The small values of the conductance steps in our measurements could be due to the low transmission coefficients or the long wire length in our sample, which was longer than the phase-breaking length L_ϕ. In other words, the transport in our wire is only partially coherent. As we know, the calculation of transmission coefficients can be done from elementary quantum mechanics if the transport is coherent, or from semiclassical Monte Carlo simulation, which is equivalent to solving the Boltzmann equation, if phase-breaking processes are so frequent that a totally incoherent transport can be assumed. However, when the transport is partially coherent as in the present case, there are no simple methods available at present. We found that, as a good approximation for our sample, the actual wire can be physically equivalent in a quantum point contact, which gives the observed quantized steps, in series with a large gate-voltage-dependent resistor, which reduces the observed total conductance and the step size. This is reasonable due to the physical width variation in the long fabricated wirelike gate[11] and has been confirmed by a scanning electron microscopy examination. The total conductance in our experiments G_{expt} should be

$$G_{\text{expt}}^{-1}=G_p^{-1}+G_s^{-1} , \tag{2}$$

where G_p is the conductance of the quantum point contact, as expressed by Eq. (1) in the adiabatic limit, and G_s is the conductance of a series resistor, which is proportional to the electron density in the inversion wire, i.e., proportional to (V_G-V_T) in the region in which we are interested. Evidence of the existence of this series resistor can be seen in Fig. 2 that the minima in the conductance derivative curve, corresponding to the quantized steps in the conductance curve, are not at zero but shifted slightly towards positive values. A simple fit of Eq. (2) to the experimental G-V_G curve in Fig. 2 (dashed line) indicates that the first conductance step corresponding to the ground state ($n=0$) is missing, and the variable series resistance is about 9.7 times[12] the corresponding point contact resistance G_p^{-1} at a certain V_G. Meanwhile, it also gives a device threshold of $V_T=2.38$ V from which the Fermi energy at different V_G can be determined, i.e.,

$$E_F=(\pi\hbar^2 N_{2D})/2m^* ,$$

where $N_{2D}=C_{\text{ox}}(V_G-V_T)/e$ is the area density of electrons under the gate. When the Fermi level is raised to the nth subband, i.e., $E_F=E_n$, the nth conductance step should be seen. The difference in V_G between any two adjacent steps, ~0.135 V, gives a nearly constant subband spacing of $\hbar w_0=0.92\pm0.005$ meV, which suggests an approximately harmonic potential confinement in our inversion wire.

We can now estimate the effective channel width of our wire MOSFET by using $W_{\text{eff}}=(8E_F/m^* w_0^2)^{1/2}$, which is 82 nm, consistent with the physical dimension of the wirelike poly-Si gate which was about 70 nm in width. An estimation of the 1D electron density $N_{1D}=C_{\text{ox}}W_{\text{eff}}(V_G-V_T)/e$ at the first measured conductance step ($G \sim 0.6e^2/h$), 2.33×10^6 cm^{-1}, confirms its correspondence to the filling of the $n=1$ subband. This figure agrees reasonably well with previous calculated results of Laux and Stern[13] on a similar structure, and indicates again the missing of a conductance step relating to the $n=0$ subband, which might be due to the existence of an impurity state related resonant tunneling peak.

To further convince ourselves of the physical picture of the wire, we tried to apply a perpendicular magnetic field to the device. The magnetic field creates edge states in the inversion wire, which reduce backscattering of electrons considerably in the incident contact of the wire, and increase the conductance as a consequence. Meanwhile, the conductance steps due to the quantum point contact become better defined, as predicted from recent theoretical calculations by Ando.[3] Such behavior was confirmed by the experiments.

On the other hand, the electron subbands of a wire can develop into hybrid magnetoelectric subbands in a magnetic field. The increasing magnetic field will increase the subband spacing, causing magnetic-field depopulation. Figure 3 shows the subband index n and $1/B$ relationship at different V_G (solid lines) as extracted from the magnetic-field-dependent conductance measurements of our inversion wire. It can be seen that, similar to results reported before,[7] our measured curves of the subband in-

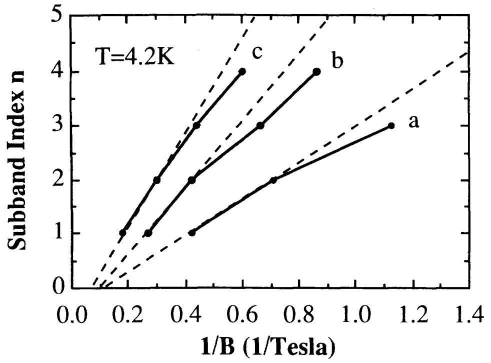

FIG. 3. The subband index n and $1/B$ relationship (solid lines) of the wire at different V_G. The pure 2D behavior is also plotted as dashed lines. Curve a, $V_G = 2.95$ V; b, $V_G = 3.10$ V; c, $V_G = 3.20$ V.

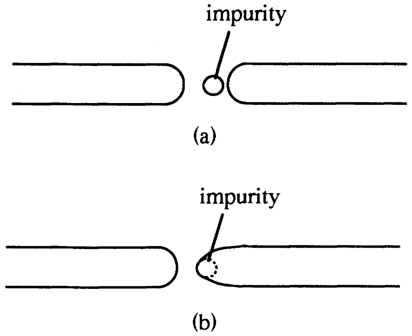

FIG. 4. Physical picture of the inversion wire. (a) The potential distribution of a quantum point contact with an isolated impurity state in the middle at $V_G < V_T$; (b) the potential distribution when the impurity state attached to one side of the quantum point contact at $V_G > V_T$.

dex n are slightly away from the corresponding 2D behavior (dashed lines in Fig. 3) at high $1/B$ indicating a 1D behavior of the wire. Using a procedure described in Ref. 7, we can estimate both the Fermi energy E_F and the subband spacing $\hbar w_0$ at each V_G by assuming a harmonic potential confinement in the wire. This process gives $\hbar w_0 = 0.93$ meV at $V_G = 2.95$ V, consistent with our previous estimation from the $G \sim V_G$ relationship in Fig. 2. A reduction of $\hbar w_0$ from 0.93 to 0.90 meV is also obtained when V_G increases from 2.95 to 3.20 V, which is attributed to the slight broadening of the effective channel width of the wire with increasing V_G.

Except for the quantized conductance discussed above, the observation of resonant tunneling through impurity states in Fig. 2 also supports our argument on the existence of a constriction or a point contact in the wire. This feature with an asymmetric profile increases its intensity with increasing magnetic field (not shown). Assuming the impurity states are due to the charge states in the oxide layer, and the charge density in our oxide is about 10^{15} m^{-2}, we can estimate the total number of charge states under the gate between the two probes $P1$ and $P2$, which is about 70. The number of impurity states within the point contact should be much less, therefore it is reasonable to assume that the impurity states are well isolated in the point contact. The potential distribution should be similar to that of a Coulomb blockade structure. Meanwhile, the asymmetric profile of the resonant tunneling peak and its magnetic-field dependence suggest that the impurity state locates closer to one side of the point contact than the other in the wire, i.e., the wire contains a localized state with a high static potential barrier to one side and a low potential barrier to the other side of the point contact [Fig. 4(a)], which constructs a full picture of the wire. When $N_{1D} < 2.2 \times 10^6$ cm^{-1},[13] the increasing V_G will not be able to force the disappearance of the lower potential barrier and only resonant tunneling through the single impurity state is possible, which explains the missing of the $n=0$ conductance step. Further increase of V_G will make the double barrier system reduce to a single point contact, which contributes to the quantization in the conductance measurements.

This work also suggests a possible way of making quantum point contacts in Si by intentionally introducing a constriction in a shorter wire, which is currently in progress.

Summarizing the above results, we can conclude that we have for the first time observed quantized conductance in a long narrow silicon inversion wire with a conductance step size of less than e^2/h, which has been explained as a result of a quantum point contact in series with a large gate-voltage-dependent wire resistor in the structure. Resonant tunneling through a single impurity state within the point contact is also detected.

The authors wish to acknowledge the Edinburgh Microfabrication Facility for processing the device, and thank A. Ross for his help with the low-temperature conductance measurements. This work was supported by the United Kingdom Science and Engineering Research Council and the Department of Trade and Industry under the silicon-2000 project.

---

[1] B. J. van Wees, H. van Houten, C. W. J. Beenakker, J. G. Williamson, L. P. Kouwenhoven, D. van der Marel, and C. T. Foxon, Phys. Rev. Lett. **60**, 848 (1988); D. A. Wharam, T. J. Thornton, R. Newbury, M. Pepper, H. Ahmed, J. E. F. Frost, D. G. Hasko, D. C. Peacock, D. A. Ritchie, and G. A. C. Jones, J. Phys. C **21**, L209 (1988).

[2] J. G. Williamson, C. E. Timmering, C. J. P. M. Harmans, J. J. Harris, and C. T. Foxon, Phys. Rev. B **42**, 7675 (1990).

[3] T. Ando, Phys. Rev. B **44**, 8017 (1991).

[4] K. Ismail, S. Washburn, and K. Y. Lee, Appl. Phys. Lett. **59**, 1998 (1991).

[5] For example, W. J. Skocpol, L. D. Jackel, R. E. Howard, H. G. Craighead, L. A. Fetter, P. M. Mankiewich, P. Grabbe, and D. M. Tennant, Surf. Sci. **142**, 14 (1984).

[6] A. C. Warren, D. A. Antoniadis, and H. I. Smith, Phys. Rev. Lett. **56**, 1858 (1986).

[7] J. R. Gao, C. de Graaf, J. Caro, S. Radelaar, M. Offenberg, V. Lauer, J. Singleton, T. J. B. M. Janssen, and J. A. A. J. Perenboom, Phys. Rev. B **41**, 12 315 (1990).

[8] P. L. McEuen, B. W. Alphenaa, R. G. Wheeler, and R. N. Sacks, Surf. Sci. **229**, 312 (1990).

[9] Y. S. Tang and C. D. W. Wilkinson, Appl. Phys. Lett. **59**, 2898 (1991); Y. S. Tang, R. Cheung, and C. D. W. Wilkinson, Electron. Lett. **26**, 1823 (1990).

[10] R. Landauer, IBM J. Res. Dev. **32**, 306 (1988).

[11] J. A. Nixon, J. H. Davies, and H. U. Baranger, Phys. Rev. B **42**, 12 638 (1991).

[12] The actual value of this series resistor can be much smaller since the real conductance of a short constriction in a wire is less than that of an ideal point contact, i.e., $G_{\text{real}}=G_p(1-\gamma)$, where $0<\gamma<1$. This effect has been observed by H. van Houten, C. W. J. Beenakker, P. H. M. van Loosdrecht, T. J. Thornton, H. Ahmed, M. Pepper, C. T. Foxon, and J. J. Harris, Phys. Rev. B **37**, 8354 (1988).

[13] S. E. Laux and F. Stern, Appl. Phys. Lett. **49**, 91 (1986).

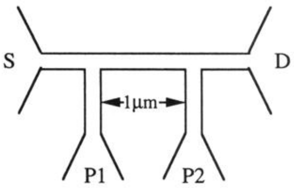

(a) top view

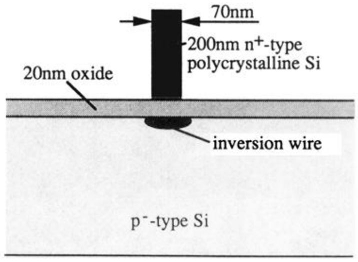

(b) cross section

FIG. 1. Schematic diagram of the device structure.